Position Error Bound for UWB Localization in Dense Cluttered Environments

DAMIEN B. JOURDAN, Member, IEEE
Athena Technologies, Inc.

DAVIDE DARDARI, Member, IEEE
University of Bologna at Cesena
Italy

MOE Z. WIN, Fellow, IEEE
Massachusetts Institute of Technology

For most outdoor applications, systems such as Global Positioning System (GPS) provide users with accurate location estimates. However, similar range-only localization techniques in dense cluttered environments typically lack accuracy and reliability due, notably, to dense multipath, line-of-sight (LOS) blockage and excess propagation delays through materials. In particular, range measurements between a receiver and a transmitter are often positively biased. Furthermore, the quality of the range measurement degrades with distance, and the geometric configuration of the beacons also affects the localization accuracy.

In this paper we derive a fundamental limit of localization accuracy for an ultrawide bandwidth (UWB) system operating in such environments, which we call the position error bound (PEB). The impact of different ranging estimation errors due to beacons distance and biases on the best positioning accuracy is investigated. The statistical characterization of biases coming from measurement campaigns can easily be incorporated into this analysis. We show that the relative importance of information coming from different beacons varies depending on the propagation conditions, such as whether the beacon is LOS or non-line-of-sight (NLOS). We show, in particular, that any a priori information knowledge on NLOS beacons can significantly improve the localization accuracy, especially in dense cluttered environments. Finally we put forth the concept of localization outage probability and ϵ-localization accuracy outage, and use them to characterize the quality of localization throughout the area.

Manuscript received March 3, 2006; revised September 1, 2006; released for publication April 12, 2007.

IEEE Log No. T-AES/44/2/926546.

Refereeing of this contribution was handled by T. F. Roome.

This research was supported, in part, by the Ministero dell'Istruzione, Universitàe della Ricerca Scientifica (MIUR) under the Virtual Immersive Communications (VICom) project, the Institute of Advanced Study Natural Science & Technology Fellowship, the Charles Stark Draper Laboratory Robust Distributed Sensor Networks Program, the Office of Naval Research Young Investigator Award N00014-03-1-0489, and the National Science Foundation under Grant ANI-0335256.

Part of the results of this research were presented at the IEEE International Conference on Communications, Istanbul, Turkey, June 2006.

Authors' current addresses: D. B. Jourdan, Athena Technologies, Inc., 6876 Watson Court Warrenton, VA 20187, Email: (jourdan@alum.mit.edu); D. Dardari, WiLAB-DEIS, University of Bologna at Cesena, via Venezia 52, Cesena (FC), Italy, E-mail: (ddardari@ieee.org); M. Z. Win, Laboratory for Information and Decision Systems, Massachusetts Institute of Technology, 77 Massachusetts Ave, Cambridge, MA, E-mail: (moewin@mit.edu).

I. INTRODUCTION

Since the Global Positioning System (GPS) became widely accessible [1], localization in the absolute frame (or geolocation) has found application in many different fields. In areas where there is a good line-of-sight (LOS) to GPS satellites, this technique provides a good estimate (within a few meters) of the user's location on the Earth. However, in indoor and dense urban environments, geolocation has always been a more challenging problem for several reasons. The GPS signal is, for example, not strong enough to penetrate through most materials. As soon as an object hides the GPS satellite from the user's view, the signal is corrupted. This constrains the usefulness of GPS to open environments, and limits its performance in forests or in dense urban environments, as retaining a lock on the GPS signals becomes more difficult. GPS typically becomes completely useless inside buildings. However there is an increasing need for accurate geolocation in cluttered environments, in addition to open spaces. In commercial applications for example, the tracking of inventory in warehouses or cargo ships is an emerging need. In military applications the problem of "blue force tracking," i.e., knowing where friendly forces are, is of vital importance, especially in urban scenarios.

To address the problem of geolocation in cluttered environments, we consider a network of fixed beacons (or anchor nodes) emitting ultrawide bandwidth (UWB) signals for ranging purposes. UWB technology potentially provides high ranging accuracy in cluttered environments [2–7] owing to its inherent delay resolution and ability to penetrate obstacles [8–13]. Further information on the fundamentals of UWB can be found in [14]–[18] and the references therein. We assume that the location of these beacons is known, for example because they are placed outside and can rely on GPS. The agent (or unknown node) estimates the ranges to these beacons to determine its position. These ranges are often obtained by estimating the time-of-arrival of the signal, for which several techniques exist [2, 3, 6, 19, 20].

The accuracy of range-only localization systems depends mainly on two factors. The first is the geometric configuration of the system, i.e., how the beacons are placed relative to the agent. The second is the quality of the range measurements themselves. If the range estimates to the beacons were perfect, then three beacons, placed at any (but distinct) locations would be sufficient to determine the agent position unambiguously in 2D, using any triangulation technique. In practice, however, these measurements are corrupted due to the propagation properties of the environment. Partial and complete LOS blockage (see Section II) lead, for example, to biased range estimates. Furthermore, the measurement variance

increases as the received signal-to-noise ratio (SNR) decreases, which is in general related to an increase in distance between agent and beacon [3]. All these factors will affect the localization accuracy to different degrees.

A measure of the localization performance used extensively in the GPS community is the geometric dilution of precision (GDOP) [1]. The GDOP provides a systematic way to compare geometric configurations of beacons. Bounds on the GDOP have also been derived in [21]. It turns out that there is a close relationship between the GDOP and the Cramér-Rao bound (CRB) from estimation theory [22, 23]. Along this line, estimation bounds for localization of sensors in a sensor network, either with or without anchor nodes, have been derived in [24]. The effect of geometric configurations and node density on the localization accuracy has been investigated in [25]. It has been shown numerically that collaborative localization, where sensors use range information not only from the anchor nodes but also from each other, is superior to localization relying solely on the anchor nodes [26].

Biases in bearing measurements are treated as additional noise with particular known a priori statistics in [27]. In [28], [29] the biases on range measurements are treated as additional parameters to be estimated for a range-only localization system. It was shown that in the absence of prior information about the biases, the non-line-of-sight (NLOS) beacons do not improve the geolocation accuracy [28], whereas if some prior information (such as their probability density function (pdf)) is available, NLOS beacons can improve it [29]. In [30], the authors investigate the improvement in positioning accuracy if all multipath delays, instead of simply the first path, are processed. It is shown that using the first arrival only is sufficient for optimal localization when no prior information is known about the NLOS delays, whereas when such prior information is available, then the multipath delays can improve the accuracy (with the drawback of a more complex receiver). These papers are restricted to particular bias models, and they do not take into account the dependence on distance of the variance of the range measurements. This dependence was addressed by numerical simulations in [26] and briefly discussed in [24]. We note that another bound was suggested in [31], and analyzed via simulations.

In this paper we derive the position error bound (PEB), a fundamental limit of localization accuracy using the information inequality [22] for the UWB localization system. This bound accounts for the dependence on distance of the range measurements and the presence of positive biases. The PEB can easily incorporate any statistical characterization of the biases, e.g., coming from measurement campaigns.

The structure of the PEB shows explicitely that the contribution in localization accuracy from each beacon is weighted by a factor reflecting the propagation environment, thereby providing insights into the importance of information coming from each beacon. In particular, it is shown that LOS beacons contribute with a larger weight than NLOS ones (at equal distance).

We quantify the importance of information from NLOS beacons to show that NLOS beacons can significantly improve the localization accuracy (provided some minimum a priori statistical knowledge of the biases) compared to the case where only LOS beacons are considered, especially in dense cluttered environments characterized by a low number of LOS beacons. Although most theoretical results are generalized to 3D, we restrict our numerical analysis to the 2D case.

The results derived thereafter are not limited to UWB ranging, however this technique is the only one able to guarantee high localization accuracy in cluttered environments. Knowing such limit can guide engineering decisions. It can also serve to map the area in terms of localization accuracy, so that the agent does not venture in locations with unsatisfactory coverage.

Finally we put forth the concept of localization accuracy outage to characterize the quality of localization throughout the area. It can be used to design the localization network in deciding how many sensors to deploy and where to place them, or when additional sensor deployment is needed [32].

The paper is organized as follows. In Section II we derive the bound for our system of UWB beacons, while in Section III we use this bound to conduct several numerical case studies. We conclude this paper in Section IV.

II. DERIVATION OF A LOWER BOUND ON THE LOCALIZATION ACCURACY

We consider a system of n_B UWB beacons used to localize a single target, or agent. We start by modeling the UWB range measurements, and then proceed to derive a lower bound on the position error for this system.

A. Modeling of Range Measurements

Let us first define a few terms. We refer to a range measurement between a transmitter and a receiver as a direct path (DP) measurement if the range is obtained from the signal traveling along a straight line between the two points. A measurement can be non-DP if the DP signal is completely obstructed. In this case, the first signal to arrive at the receiver may come from reflected paths only. An LOS measurement is one obtained when the signal travels along an

unobstructed DP, while an NLOS measurement can come from complete DP blockage or DP excess delay (in the latter case the DP is partially obstructed so that the signal has to traverse different materials, which results in additional delays).

In the case of radio-based localization, range measurements are typically corrupted by four sources: multipath fading, thermal noise, DP blockage, and DP excess delay. Multipath fading is due to destructive and constructive interference of signals arriving at the receiver via different propagation paths. This makes the detection of DP, if present, challenging. However UWB signals have the capability to resolve multipath components, which greatly reduce multipath fading [8–11]. The presence of thermal noise also limits the ability to accurately determine ranges as the distance increases, i.e., as the SNR decreases. We account for this effect by introducing a suitable model for the variance of the range measurements error as a function of the beacons distance [6, 3].

The third difficulty is due to DP blockage. In some areas of the environment the DP to certain beacons may be completely obstructed, so that the only received signals are from reflections, resulting in measured ranges larger than the true distances. The fourth difficulty is due to DP excess delay incurred by propagation of the partially obstructed DP through different materials, such as walls. When such a partially obstructed DP signal is observed as first arrival, the propagation time depends not only upon the traveled distance, but also upon the materials it encountered. Because the propagation of electromagnetic signals is slower in some materials than in the air, the signal arrives with excess delay, yielding again a range estimate larger than the true one. An important observation is that the effect of DP blockage and DP excess delay is the same: they both add a positive bias to the true range between agent and beacon, so that the measured range is larger than the true value (from now on we therefore refer to such measurements as NLOS). This positive error has been identified as a limiting factor in UWB ranging performance [7, 3], so it must be accounted for.

In our system, the range measurements $\tilde{r}_i$ between the agent and the ith beacon can therefore be positively biased due to NLOS propagation. If we denote by d_i the true distance, the measured range $\tilde{r}_i$ can be expressed as

$$\tilde{r}_i = d_i + b_i + \epsilon_i \tag{1}$$

where b_i is the bias added to the ith beacon and ϵ_i is a random Gaussian noise, independent of b_i, with zero-mean and variance σ_i^2. Following the analysis found in [6], [10], we model the dependence of the variance of ϵ_i on the distance d_i as $\sigma_i^2 \equiv \sigma^2(d_i) = \sigma_0^2 d_i^\alpha$, where α is the path-loss exponent and σ_0^2 is the variance at 1 m. The pdf of ϵ_i is therefore:

$$f_{\epsilon_i}(\epsilon) = \frac{1}{\sqrt{2\pi}\sigma(d_i)} e^{-\epsilon^2/2\sigma^2(d_i)}. \tag{2}$$

Let us now model the statistics of the bias.

In most applications it is unrealistic to assume a perfect knowledge of the bias; in that case it could be simply subtracted from the range measurement. A more realistic option is to consider some a priori statistical characterization derived from measurements or induced from the environment configuration.

Let us start by making some general observations about the biases using real data from UWB range measurements. From the results presented in [33] it can be concluded that the bias will always be nonnegative. Its actual value, however, will largely depend on the environment. We expect it to take a wider range of values in a cluttered environment with many walls, machines, and furniture (such as a typical office building), than in an open space. Indeed actual UWB range measurements performed in an office environment in [33], [2] show that the bias jumps from one value to another as the transmitter is moved through the building. In [33] the bias is seen to vary between 0 and 1.5 m, depending on the room in which the measurements were taken. Note finally that the bias cannot grow infinitely large, regardless of the propagation environment.

Although a detailed map of the environment may not be available, most of the time we will be able to classify the environment in broad terms, such as "concrete office building," or "wooden warehouse" (which we call an environment class). By performing range measurements in typical buildings of different classes beforehand, we can build a library of frequency histograms valid for different environments classes. We can then use these histograms to approximate the pdf of the biases in the building of interest. An example of such histogram is derived from [33], where range measurements were performed at different locations in the corridor of an office building. The corresponding frequency histogram of the bias is plotted on Fig. 1(a). Such histograms account for the positivity of the biases, as well as an approximate distribution of their expected value throughout the building. From Fig. 1 a we can see that biases around 0.5 m are most common, while they were never larger than 1.1 m.

Let us assume such frequency histograms are available for each beacon. They may differ from beacon to beacon, so we index them by the beacon number i. The ith histogram has $K^{(i)}$ bars, where the kth bar goes from $\beta_{k-1}^{(i)}$ to $\beta_k^{(i)}$ and has frequency (height) $p_k^{(i)}$, as shown on Fig. 1(a). We can therefore associate to the frequency histogram the pdf of b_i as

$$f_{b_i}(b) = \sum_{k=1}^{K^{(i)}} w_k^{(i)} u_{\{\beta_{k-1}^{(i)}, \beta_k^{(i)}\}}(b) \tag{3}$$

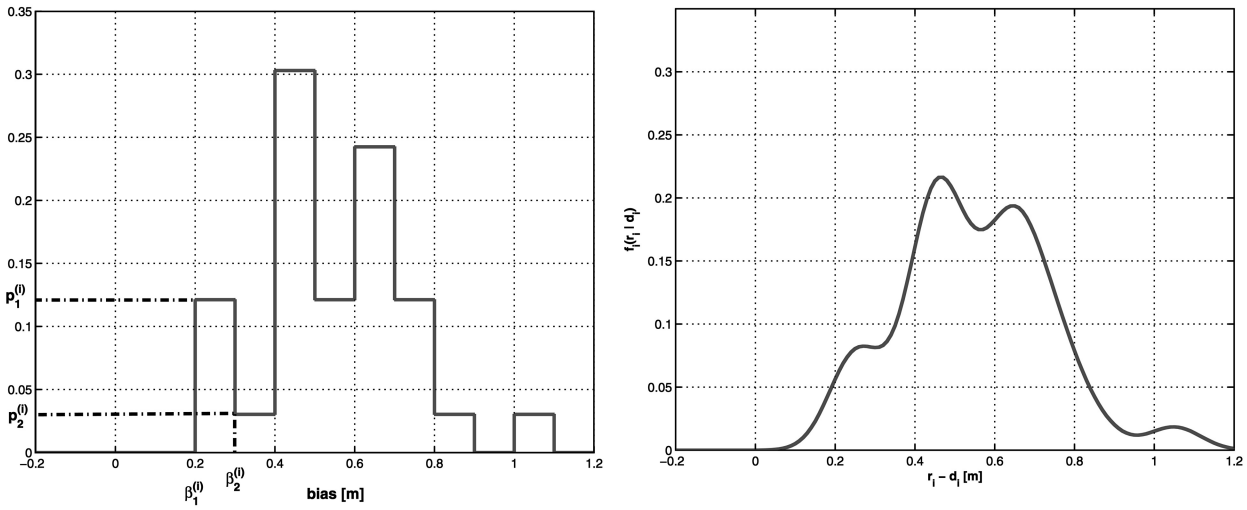

(a) (b)

Fig. 1. (a) Frequency histogram of bias from range measurements performed in office building [33]. (b) Corresponding pdf of error in range measurements $\tilde{r}_i - d_i$ from beacon i, for $d_i = 15$ m and $\sigma_0 = 10^{-3}$ m.

where $w_k^{(i)} = p_k^{(i)}/(\beta_k^{(i)} - \beta_{k-1}^{(i)})$, $u_{\{a,a'\}}(b) = 1$ if $a \le b \le a'$, 0 otherwise, and $\beta_0^{(i)} = 0$. We note that if beacon i is LOS (i.e., it has no bias), then $f_{b_i}(b) = \delta(b)$ where $\delta(b)$ is the Dirac pseudo function. In any case, even in absence of measured data, given a fixed scenario we can always determine the maximum expected bias β_{m} and, in absence of other a priori information, assume a uniform distribution in $[0, \beta_{\mathrm{m}}]$, i.e., $K = 1$, $\beta_1 = \beta_{\mathrm{m}}$, and $w_1 = 1/\beta_{\mathrm{m}}$.

In [29] the biases are treated as additional parameters to be estimated. However it can be shown that if the biases are modeled as described above, this approach fails to yield a bound lower than that when the NLOS beacons are ignored. In this paper we instead treat the biases as additional noise terms on the range estimate, and we show that a better performance limit can be obtained, as the information from NLOS beacons can help improve the accuracy bound.

Let us then lump the bias term with the Gaussian measurement noise $\tilde{\nu}_i = b_i + \epsilon_i$ and obtain the corresponding pdf:

$$f_{\tilde{\nu}_i}(\tilde{\nu}_i) = \int_{-\infty}^{\infty} f_{b_i}(x) f_{\epsilon_i}(\tilde{\nu}_i - x)\,dx \tag{4}$$

$$= \sum_{k=1}^{K^{(i)}} w_k^{(i)} \int_{\beta_{k-1}^{(i)}}^{\beta_k^{(i)}} f_{\epsilon_i}(\tilde{\nu}_i - x)\,dx \tag{5}$$

$$= \sum_{k=1}^{K^{(i)}} w_k^{(i)} \left[Q\left(\frac{\tilde{\nu}_i - \beta_k^{(i)}}{\sigma(d_i)} \right) - Q\left(\frac{\tilde{\nu}_i - \beta_{k-1}^{(i)}}{\sigma(d_i)} \right) \right] \tag{6}$$

where $Q(x) = (1/\sqrt{2\pi}) \int_x^{+\infty} e^{-t^2/2} dt$ is the Gaussian Q function. If the ith beacon is LOS, then ν_i is Gaussian distributed with zero mean and variance $\sigma^2(d_i)$. The mean of $\tilde{\nu}_i$ is denoted m_i, and in order to obtain an unbiased estimator we subtract m_i from the ith range measurement. This is equivalent to replace $\tilde{\nu}_i$ by $\nu_i \triangleq \tilde{\nu}_i - m_i$. Let $\mathbf{p}_{\mathrm{A}} = (x_{\mathrm{A}}, y_{\mathrm{A}})$ be the vector of the agent's coordinates so that

$$d_i(\mathbf{p}_{\mathrm{A}}) = \sqrt{(x_{\mathrm{A}} - x_i)^2 + (y_{\mathrm{A}} - y_i)^2}, \quad i = 1, \ldots, n_{\mathrm{B}} \tag{7}$$

where (x_i, y_i) are the coordinates of the ith beacon, assumed to be known. The unbiased range measurements are therefore modeled as

$$r_i = d_i(\mathbf{p}_{\mathrm{A}}) + \nu_i \tag{8}$$

with pdf given by

$$f_i(r_i \mid \mathbf{p}_{\mathrm{A}}) = \sum_{k=1}^{K^{(i)}} w_k^{(i)} \left[Q\left(\frac{r_i - d_i(\mathbf{p}_{\mathrm{A}}) + m_i - \beta_k^{(i)}}{\sigma(d_i(\mathbf{p}_{\mathrm{A}}))} \right) - Q\left(\frac{r_i - d_i(\mathbf{p}_{\mathrm{A}}) + m_i - \beta_{k-1}^{(i)}}{\sigma(d_i(\mathbf{p}_{\mathrm{A}}))} \right) \right]. \tag{9}$$

The pdf corresponding to the bias profile of Fig. 1(a) is plotted on Fig. 1(b) as a function of the error in range measurement $\tilde{r}_i - d_i$ for $d_i = 15$ m and $\sigma_0 = 10^{-3}$ m.

B. Position Error Bound

A lower bound on the covariance of any position estimator $\hat{\mathbf{p}}_{\mathrm{A}} = (\hat{x}_{\mathrm{A}}, \hat{y}_{\mathrm{A}})$ based on $\mathbf{r} = [r_1, r_2, \ldots, r_{n_{\mathrm{B}}}]$, the vector of n_{B} range measurements, is given by

the information inequality (or the Cramér-Rao lower bound) [22][1]:

$$\mathbb{E}_{\mathbf{r}}\{(\mathbf{p}_{\mathrm{A}}-\hat{\mathbf{p}}_{\mathrm{A}})(\mathbf{p}_{\mathrm{A}}-\hat{\mathbf{p}}_{\mathrm{A}})^{\mathrm{T}}\}\geq\mathbf{J}^{-1} \tag{10}$$

where $\mathbf{J}$ is the Fisher information matrix (FIM) given by

$$\mathbf{J}=\mathbb{E}_{\mathbf{r}}\{[\nabla_{\mathbf{p}_{\mathrm{A}}}\ln(f(\mathbf{r}\mid\mathbf{p}_{\mathrm{A}}))][\nabla_{\mathbf{p}_{\mathrm{A}}}\ln(f(\mathbf{r}\mid\mathbf{p}_{\mathrm{A}}))]^{\mathrm{T}}\} \tag{11}$$

and $f(\mathbf{r}\mid\mathbf{p}_{\mathrm{A}})$ is the pdf of the vector $\mathbf{r}$ conditioned on $\mathbf{p}_{\mathrm{A}}$, and $\nabla_{\mathbf{p}_{\mathrm{A}}}\{.\}$ denotes the gradient of a scalar with respect to $\mathbf{p}_{\mathrm{A}}$. Note that we have

$$\sqrt{\mathbb{E}_{\mathbf{r}}\{(x_{\mathrm{A}}-\hat{x}_{\mathrm{A}})^2+(y_{\mathrm{A}}-\hat{y}_{\mathrm{A}})^2\}}\geq\sqrt{\mathbb{T}\{\mathbf{J}^{-1}\}} \tag{12}$$

for any estimator of the position $\mathbf{p}_{\mathrm{A}}=(x_{\mathrm{A}},y_{\mathrm{A}})$, where $\mathbb{T}\{.\}$ is the trace of a square matrix. In the remaining we refer to this expression as the PEB:

$$\mathrm{PEB}(x_{\mathrm{A}},y_{\mathrm{A}})\triangleq\sqrt{\mathbb{T}\{\mathbf{J}^{-1}\}}. \tag{13}$$

The PEB is a fundamental limit on the accuracy of any localization method.

C. Derivation of FIM

We now seek to calculate the FIM for our system. Because the measurements are assumed to be independent we have

$$f(\mathbf{r}\mid\mathbf{p}_{\mathrm{A}})=\prod_{i=1}^{n_{\mathrm{B}}}f_i(r_i\mid\mathbf{p}_{\mathrm{A}}) \tag{14}$$

where $f_i(r_i\mid\mathbf{p}_{\mathrm{A}})$ is given by (9). We have

$$\nabla_{\mathbf{p}_{\mathrm{A}}}\ln(f(\mathbf{r}\mid\mathbf{p}_{\mathrm{A}}))=\sum_{i=1}^{n_{\mathrm{B}}}\frac{1}{f_i(r_i\mid\mathbf{p}_{\mathrm{A}})}\begin{bmatrix}\dfrac{\partial f_i(r_i\mid\mathbf{p}_{\mathrm{A}})}{\partial x_{\mathrm{A}}}\\[2ex]\dfrac{\partial f_i(r_i\mid\mathbf{p}_{\mathrm{A}})}{\partial y_{\mathrm{A}}}\end{bmatrix} \tag{15}$$

so that

$$\mathbf{J}=\mathbb{E}_{\mathbf{r}}\left\{\sum_{i=1}^{n_{\mathrm{B}}}\sum_{j=1}^{n_{\mathrm{B}}}\frac{1}{f_i(r_i\mid\mathbf{p}_{\mathrm{A}})}\frac{1}{f_j(r_j\mid\mathbf{p}_{\mathrm{A}})}\times\begin{bmatrix}\dfrac{\partial f_i(r_i\mid\mathbf{p}_{\mathrm{A}})}{\partial x_{\mathrm{A}}}\cdot\dfrac{\partial f_j(r_j\mid\mathbf{p}_{\mathrm{A}})}{\partial x_{\mathrm{A}}} & \dfrac{\partial f_i(r_i\mid\mathbf{p}_{\mathrm{A}})}{\partial x_{\mathrm{A}}}\cdot\dfrac{\partial f_j(r_j\mid\mathbf{p}_{\mathrm{A}})}{\partial y_{\mathrm{A}}}\\[2ex]\dfrac{\partial f_i(r_i\mid\mathbf{p}_{\mathrm{A}})}{\partial y_{\mathrm{A}}}\cdot\dfrac{\partial f_j(r_j\mid\mathbf{p}_{\mathrm{A}})}{\partial x_{\mathrm{A}}} & \dfrac{\partial f_i(r_i\mid\mathbf{p}_{\mathrm{A}})}{\partial y_{\mathrm{A}}}\cdot\dfrac{\partial f_j(r_j\mid\mathbf{p}_{\mathrm{A}})}{\partial y_{\mathrm{A}}}\end{bmatrix}\right\}. \tag{16}$$

[1]The notation $\mathbb{E}_{\mathbf{r}}\{.\}$ denotes the expectation operator with respect to the random variable $\mathbf{r}$, the notation $V\geq W$ means that the matrix $V-W$ is positive semi-definite, and superscript $^{\mathrm{T}}$ denotes the transpose.

We show in the Appendix that all the terms in (16) for which $i\neq j$ are 0. We therefore have

$$\mathbf{J}=\mathbb{E}_{\mathbf{r}}\left\{\sum_{i=1}^{n_{\mathrm{B}}}\frac{1}{f_i(r_i\mid\mathbf{p}_{\mathrm{A}})^2}\times\begin{bmatrix}\left(\dfrac{\partial f_i(r_i\mid\mathbf{p}_{\mathrm{A}})}{\partial x_{\mathrm{A}}}\right)^2 & \dfrac{\partial f_i(r_i\mid\mathbf{p}_{\mathrm{A}})}{\partial x_{\mathrm{A}}}\dfrac{\partial f_i(r_i\mid\mathbf{p}_{\mathrm{A}})}{\partial y_{\mathrm{A}}}\\[2ex]\dfrac{\partial f_i(r_i\mid\mathbf{p}_{\mathrm{A}})}{\partial y_{\mathrm{A}}}\dfrac{\partial f_i(r_i\mid\mathbf{p}_{\mathrm{A}})}{\partial x_{\mathrm{A}}} & \left(\dfrac{\partial f_i(r_i\mid\mathbf{p}_{\mathrm{A}})}{\partial y_{\mathrm{A}}}\right)^2\end{bmatrix}\right\}. \tag{17}$$

After a few algebraic manipulations we obtain

$$\frac{\partial f_i(r_i\mid\mathbf{p}_{\mathrm{A}})}{\partial x_{\mathrm{A}}}=g_i(\nu_i)\cos\theta_i \tag{18}$$

$$\frac{\partial f_i(r_i\mid\mathbf{p}_{\mathrm{A}})}{\partial y_{\mathrm{A}}}=g_i(\nu_i)\sin\theta_i \tag{19}$$

where θ_i is the angle between the agent and the ith beacon measured with respect to the horizontal, $\nu_i=r_i-d_i$, and $g_i(\nu_i)$ is given by

$$g_i(\nu_i)\triangleq\frac{1}{\sigma_0 d_i^{\alpha/2}\sqrt{2\pi}}\sum_{k=1}^{K^{(i)}}w_k^{(i)}\times\left[\left(1+\frac{\alpha}{2d_i}(\nu_i+m_i-\beta_k^{(i)})\right)e^{-(\nu_i+m_i-\beta_k^{(i)})^2/2\sigma_0^2 d_i^{\alpha}}-\left(1+\frac{\alpha}{2d_i}(\nu_i+m_i-\beta_{k-1}^{(i)})\right)e^{-(\nu_i+m_i-\beta_{k-1}^{(i)})^2/2\sigma_0^2 d_i^{\alpha}}\right]. \tag{20}$$

We finally obtain

$$\mathbf{J}=\sum_{i=1}^{n_{\mathrm{B}}}A(\boldsymbol{\beta}^{(i)},d_i)\mathrm{M}(\theta_i) \tag{21}$$

with $\boldsymbol{\beta}^{(i)}\triangleq\{\beta_1^{(i)},\ldots,\beta_{K^{(i)}}^{(i)}\}$,

$$\mathrm{M}(\theta)\triangleq\begin{bmatrix}\cos^2\theta & \cos\theta\sin\theta\\ \cos\theta\sin\theta & \sin^2\theta\end{bmatrix} \tag{22}$$

and

$$A(\boldsymbol{\beta}^{(i)},d_i)\triangleq\int_{-\infty}^{\infty}\frac{g_i(\nu_i)^2}{f_i(r_i\mid\mathbf{p}_{\mathrm{A}})}d\nu_i. \tag{23}$$

The expression (21) provides us with some useful insights. First, note that $\mathrm{M}(\theta_i)$ contains geometric information about the relative position of the agent with respect to the ith beacon. The FIM is therefore a weighted sum of this geometric information, where the weights $A(\boldsymbol{\beta}^{(i)},d_i)$ depend on $\boldsymbol{\beta}^{(i)}$ and d_i. We show in Section IID that these weights correspond to the importance of the information coming from the corresponding beacon, in the sense of how much new information is brought by this beacon.

We also note that our analysis can easily be extended to 3D. If the position vector $\mathbf{p}_{\mathrm{A}}$ is a 3D

vector, we define λ as its longitude (angle between the x axis and the projection of $\mathbf{p}_A$ on the x-y plane) and ϕ as its latitude (angle between the projection of $\mathbf{p}_A$ on the x-y plane and $\mathbf{p}_A$). Then (18) and (19) become

$$\frac{\partial f_i(r_i \mid \mathbf{p}_A)}{\partial x_A} = g_i(\nu_i)\cos\lambda_i\cos\phi_i \tag{24}$$

$$\frac{\partial f_i(r_i \mid \mathbf{p}_A)}{\partial y_A} = g_i(\nu_i)\sin\lambda_i\cos\phi_i \tag{25}$$

$$\frac{\partial f_i(r_i \mid \mathbf{p}_A)}{\partial z_A} = g_i(\nu_i)\sin\phi_i \tag{26}$$

where $g_i(\nu_i)$ is given by (20). The only change from (21), (22), and (23) is in the matrix $\mathrm{M}(\theta)$ which now becomes

$$\mathrm{M}(\lambda,\phi) = \begin{bmatrix} \cos^2\lambda\cos^2\phi & \cos\lambda\sin\lambda\cos^2\phi & \cos\lambda\cos\phi\sin\phi \\ \cos\lambda\sin\lambda\cos^2\phi & \sin^2\lambda\cos^2\phi & \sin\lambda\cos\phi\sin\phi \\ \cos\lambda\cos\phi\sin\phi & \sin\lambda\cos\phi\sin\phi & \sin^2\phi \end{bmatrix}. \tag{27}$$

D. Analysis of Weights $A(\boldsymbol{\beta},d)$

Let us investigate the behavior of $A(\boldsymbol{\beta},d)$ as a function of $\boldsymbol{\beta}$ and d. As a sanity check let us first consider the case when all the biases go to 0, with d fixed. This implies that the β_k tend to 0 for all k, and that the mean of the corresponding measurement noise m also goes to 0, according to (6). We write this as $m-\boldsymbol{\beta}\to 0$. We then have the following first-order approximation for small $m-\beta_k$:

$$Q\left(\frac{\nu}{\sigma}+\frac{m-\beta_k}{\sigma}\right) = Q\left(\frac{\nu}{\sigma}\right) - \frac{m-\beta_k}{\sigma\sqrt{2\pi}}e^{-\nu^2/2\sigma^2} + o(m-\beta_k) \tag{28}$$

$$e^{-(\nu+m-\beta_k)^2/2\sigma^2} = \left(1-(m-\beta_k)\frac{\nu}{\sigma^2}\right)e^{-\nu^2/2\sigma^2} + o(m-\beta_k). \tag{29}$$

We use these to calculate the limit of (9) when $m-\boldsymbol{\beta}\to 0$:

$$\lim_{m-\boldsymbol{\beta}\to 0} f(r \mid \mathbf{p}_A) = \lim_{m-\boldsymbol{\beta}\to 0}\sum_{k=1}^{K} w_k\left[Q\left(\frac{\nu+m-\beta_k}{\sigma(d)}\right) - Q\left(\frac{\nu+m-\beta_{k-1}}{\sigma(d)}\right)\right] \tag{30}$$

$$= \lim_{m-\boldsymbol{\beta}\to 0}\sum_{k=1}^{K} w_k\left[-\frac{m-\beta_k}{\sigma(d)\sqrt{2\pi}} + \frac{m-\beta_{k-1}}{\sigma(d)\sqrt{2\pi}}\right]e^{-\nu^2/2\sigma^2(d)} \tag{31}$$

$$= \frac{1}{\sigma(d)\sqrt{2\pi}}e^{-\nu^2/2\sigma^2(d)}\lim_{m-\boldsymbol{\beta}\to 0}\sum_{k=1}^{K} w_k(\beta_k-\beta_{k-1}) \tag{32}$$

$$= \frac{1}{\sigma(d)\sqrt{2\pi}}e^{-\nu^2/2\sigma^2(d)} \tag{33}$$

where we have used the fact that $\sum_{k=1}^{K} w_k(\beta_k-\beta_{k-1}) = 1$. The pdf of the range measurements converges to a zero-mean Gaussian of variance $\sigma^2(d)$, as expected. We now look at the limit of $g(\nu)$. We have

$$\lim_{m-\beta\to 0}\left(1+\frac{\alpha}{2d}(\nu+m-\beta)\right)e^{-(\nu+m-\beta)^2/2\sigma^2} = e^{-\nu^2/2\sigma^2}\lim_{m-\beta\to 0}\left(1+\frac{\alpha}{2d}\nu+(m-\beta)\left(\frac{\alpha}{2d}-\frac{\nu}{\sigma^2}-\frac{\alpha\nu^2}{2d\sigma^2}\right)\right) \tag{34}$$

so that

$$\lim_{m-\beta\to 0} g(\nu) = \frac{1}{\sigma(d)\sqrt{2\pi}}e^{-\nu^2/2\sigma^2(d)}\lim_{m-\beta\to 0}\sum_{k=1}^{K} w_k \times\left[\left(\frac{\alpha}{2d}-\frac{\nu}{\sigma^2(d)}-\frac{\alpha\nu^2}{2d\sigma^2(d)}\right)(\beta_{k-1}-\beta_k)\right] \tag{35}$$

$$= \frac{1}{\sigma(d)\sqrt{2\pi}}\left(\frac{\alpha\nu^2}{2d\sigma^2(d)}+\frac{\nu}{\sigma^2(d)}-\frac{\alpha}{2d}\right)e^{-\nu^2/2\sigma^2(d)}. \tag{36}$$

We can then calculate $A(\boldsymbol{\beta},d)$ when $\boldsymbol{\beta}$ is 0. If we let $y=\nu/\left(\sigma(d)\sqrt{2}\right)$, we obtain

$$A(0,d) = \frac{1}{\sqrt{\pi}}\int_{-\infty}^{\infty}\left(\frac{\alpha}{d}y^2+\frac{\sqrt{2}}{\sigma(d)}y-\frac{\alpha}{2d}\right)^2 e^{-y^2}dy \tag{37}$$

$$= \frac{1}{\sqrt{\pi}}\left[\frac{\alpha^2}{d^2}\int_{-\infty}^{\infty}y^4e^{-y^2}dy+\left(\frac{2}{\sigma^2(d)}-\frac{\alpha^2}{d^2}\right)\times\int_{-\infty}^{\infty}y^2e^{-y^2}dy+\frac{\alpha^2}{4d^2}\int_{-\infty}^{\infty}e^{-y^2}dy\right] \tag{38}$$

$$= \frac{1}{\sqrt{\pi}}\left[\frac{\alpha^2}{d^2}\frac{3\sqrt{\pi}}{4}+\left(\frac{2}{\sigma^2(d)}-\frac{\alpha^2}{d^2}\right)\frac{\sqrt{\pi}}{2}+\frac{\alpha^2}{4d^2}\sqrt{\pi}\right] \tag{39}$$

$$= \frac{1}{\sigma^2(d)}+\frac{\alpha^2}{2d^2}. \tag{40}$$

In the following we consider the particular case where the biases are uniformly distributed between 0 and β_m, with the purpose of emphasizing in a simple way the role played by the NLOS beacons when the biases grow. As already mentioned, it can also model the case where all that is known about the environment is that the bias cannot be greater than β_m. The corresponding pdf (9) is plotted on Fig. 2. In this case the weights $A(\beta_m,d)$ are equal to

$$A(\beta_m,d) = \frac{1}{\beta_m\sigma(d)\pi\sqrt{2}}\int_{-\infty}^{\infty}h(y,\beta_m,d)dy \tag{41}$$

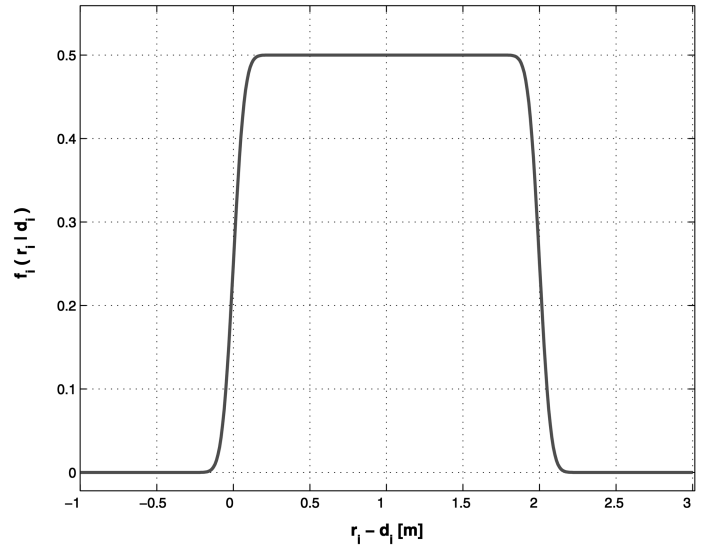

Fig. 2. Pdf of error in range measurements $\tilde{r}_i - d_i$ when $K^{(i)} = 1$, given true distance $d_i = 15$ m and $\beta^{(i)} = \beta_{\mathrm{m}} = 2$ m.

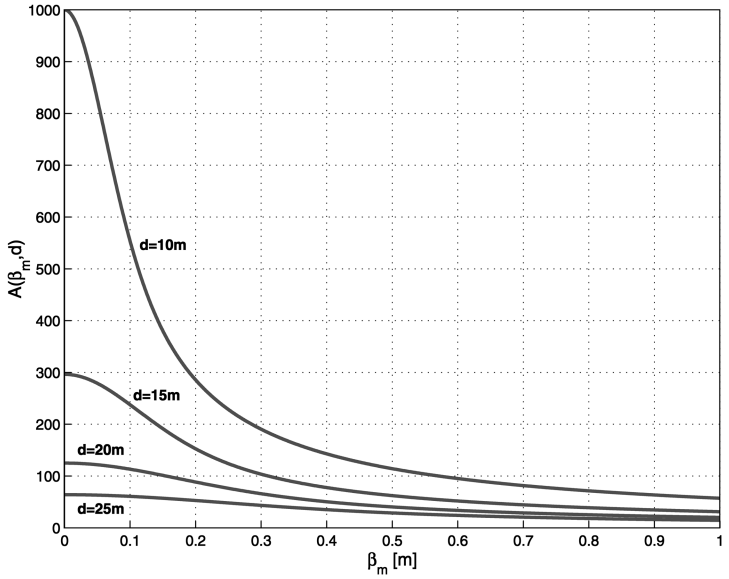

Fig. 3. $A(\beta_{\mathrm{m}},d)$ for several values of d in the case where $\sigma_0 = 0.001$ m and $\alpha = 3$.

where

$$h(y,\beta,d) = \frac{\left[\left(e^{-y^2} - e^{-\left(y+(\beta/\sigma(d)\sqrt{2})\right)^2}\right)\left(1 + \dfrac{\alpha\sigma(d)}{d\sqrt{2}}y\right) - \dfrac{\alpha\beta}{2d}e^{-\left(y+(\beta/\sigma(d)\sqrt{2})\right)^2}\right]^2}{Q\left(\sqrt{2}y\right) - Q\left(\sqrt{2}y + \dfrac{\beta}{\sigma(d)}\right)}. \tag{42}$$

We now turn our attention to the case when the biases grow to infinity. When $\beta_{\mathrm{m}} \to +\infty$ for a given d, the integral in (41) tends to a constant so that we have

$$A(\beta_{\mathrm{m}},d) \sim \frac{1}{\beta_{\mathrm{m}}} \quad \text{when} \quad \beta_{\mathrm{m}} \to +\infty. \tag{43}$$

For a given d, $A(\beta_{\mathrm{m}},d)$ therefore approaches 0 as β_{m} goes to infinity. From (40) we see that the same is true when d goes to infinity (so that the range estimation variance goes to infinity). This is consistent with our intuition that the larger the bias or the range estimation variance, the less valuable the corresponding range information will be in determining the agent's position: the corresponding $\mathrm{M}(\theta)$ in (21) will receive a low weight and the contribution from the ith beacon will be small. The weights $A(\beta^{(i)},d_i)$ therefore quantify the importance of the information coming from the ith beacon. This implies that the information from beacons that are far away (large range measurement variance) or that are in highly cluttered areas (large bias) will not contribute much to the FIM. This behavior is illustrated on Fig. 3, where we used (41) to plot

$A(\beta_m, d)$ as a function of β_m, for several values of d. It can be seen that when d is small, the weights are sensitive to changes in β_m. Indeed at short distances the variance $\sigma^2(d)$ of the Gaussian noise is small, and therefore the dominating term in measurement inaccuracy is the bias value. However as the distance increases, the value of β_m is less significant since the large $\sigma^2(d)$ tends to dominate the error. In any case, as d or β_m increase, the importance of the information coming from the corresponding beacon decreases.

Consider a mix of LOS (for which $\beta_m^{(LOS)} = 0$) and NLOS beacons with no a priori knowledge of their biases (the biases can take any nonnegative value so they have no upper bound, or $\beta_m^{(NLOS)} \to +\infty$). Then the information from the NLOS beacons is not used at all in the calculation of the PEB since $\lim_{\beta_m \to +\infty} A(\beta_m, d) = 0$. This observation is consistent with [28], in which it was shown that in the presence of a mix of LOS and NLOS beacons (with no a priori knowledge about the NLOS statistics), the performance depends only on the LOS beacons. Our result shows however that in the case where a priori knowledge of the NLOS beacon biases is available (which is always the case since biases cannot be infinitely large), the NLOS beacons should indeed be taken into account since they contribute to the PEB. In Section III it will be shown that the contribution from NLOS beacons can be quite significant.

E. Analytical Expression for PEB

We now use the analytical expression for the FIM to obtain the PEB in (13). Recall from (21) that the FIM is a 2×2 matrix, so its inverse is easily obtained as

$$\mathbf{J}^{-1} = \frac{1}{\det \mathbf{J}} \begin{bmatrix} \sum_{i=1}^{n_B} A_i s_i^2 & -\sum_{i=1}^{n_B} A_i c_i s_i \\ -\sum_{i=1}^{n_B} A_i c_i s_i & \sum_{i=1}^{n_B} A_i c_i^2 \end{bmatrix} \tag{44}$$

where $A_i = A(\beta^{(i)}, d_i)$, $c_i = \cos\theta_i$, and $s_i = \sin\theta_i$. The PEB is then equal to

$$\mathrm{PEB}(x_A, y_A) = \sqrt{\frac{\sum_{i=1}^{n_B} A_i}{\left(\sum_{i=1}^{n_B} A_i c_i^2\right)\left(\sum_{i=1}^{n_B} A_i s_i^2\right) - \left(\sum_{i=1}^{n_B} A_i c_i s_i\right)^2}}. \tag{45}$$

We can also expand the denominator to obtain the alternate expression:

$$\mathrm{PEB}(x_A, y_A) = \sqrt{\frac{\sum_{i=1}^{n_B} A_i}{\sum_{i<j} A_i A_j \sin^2(\theta_j - \theta_i)}}. \tag{46}$$

We stress that the limit on the localization accuracy given in (45) and (46) depends on the distance between the agent and the beacons, as well as on the presence of biases. If the variance were not dependent on the distance ($\alpha = 0$) and if no bias were present ($\beta^{(i)} = 0$ for all i), then according to (40) $A_i = 1/\sigma_0^2$ for all i and the PEB is equal to

$$\mathrm{PEB}(x_A, y_A) = \sigma_0 \sqrt{\frac{n_B}{\left(\sum_{i=1}^{n_B} c_i^2\right)\left(\sum_{i=1}^{n_B} s_i^2\right) - \left(\sum_{i=1}^{n_B} c_i s_i\right)^2}} \tag{47}$$

which is the product of the measurement standard deviation σ_0 and the GDOP. This is the case most commonly treated in the literature for range-only localization [28, 25, 23].

III. NUMERICAL CASE STUDIES

We consider a set of n_B beacons where n_{LOS} of them are LOS, while the remaining $n_{NLOS} = n_B - n_{LOS}$ are NLOS. For the sake of these case studies we assume we know whether a beacon is LOS or NLOS (if a map of the environment is available, channel modeling tools can be used [34], otherwise NLOS identification techniques exist [35–37]). We note that in practical applications it may be more realistic to assign each beacon with a probability of being LOS and NLOS. Our analysis can be easily extended to this case.

We call ρ the fraction of LOS beacons, that is $\rho = n_{LOS}/n_B$. Typically LOS beacons have no bias so $\beta^{(i)} = 0$ for $i = 1, \ldots, n_{LOS}$. We assume that LOS beacons are placed such that they are visible from any location in the area. On the other hand we assume that all the biases related to NLOS beacons are uniformly distributed between 0 and β_m, i.e., $\beta^{(i)} = \beta_m$ for $i = n_{LOS} + 1, \ldots, n_b$. This value will vary from building to building depending on whether the environment is highly cluttered or not.

We acknowledge that assuming that beacons remain LOS or NLOS irrespective of the agent's position is not quite realistic, but our goal in the following case studies is to understand the general behavior of the PEB as we vary some key parameters in a simple scenario. The analysis of the previous sections is perfectly amenable to cases where beacons are LOS and NLOS depending on the agent's location.

The following case studies are carried out with $\alpha = 3$ (a typical value for UWB indoor environments [10]) and $\sigma_0 = 10^{-3}$ m (derived from the experimental data described in [33]).

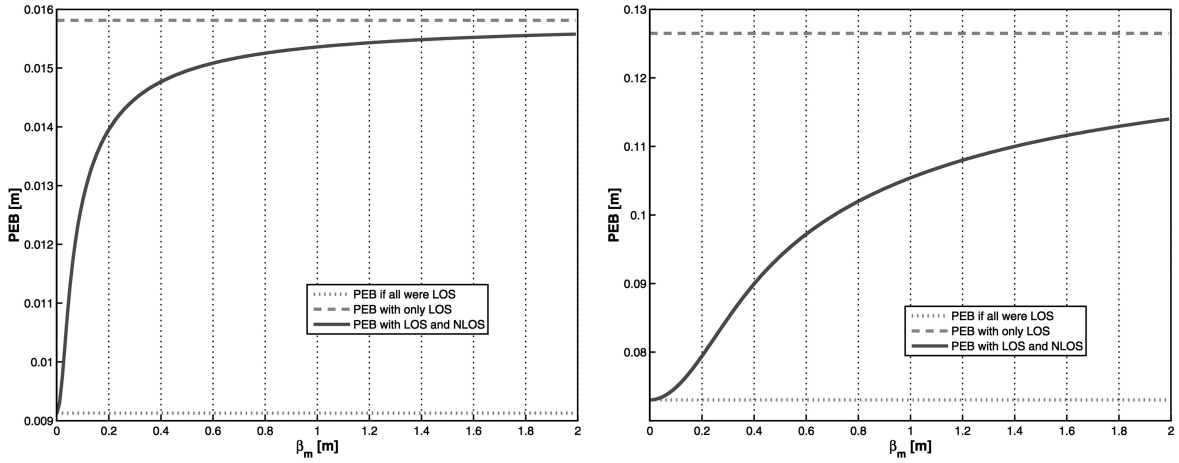

Fig. 4. Case 1 when $d = 5$ m (left), and $d = 20$ m: PEB as function of β_m (solid), bounded below by PEB when all 6 sensors are LOS (dotted), and above by PEB when only the 3 LOS beacons are considered (dashed). Lower values of PEB indicate a better localization accuracy.

A. Case Study 1: Importance of NLOS Beacons

We first consider 6 beacons placed at the vertices of a polygon of radius $d = 5$ m and 20 m, and we assume that 3 beacons are LOS, while the 3 others are NLOS (therefore $\rho = 0.5$) with a common maximum bias β_m. We plot PEB at the center of the polygon as a function of d and varying β_m from 0 to 2 m (solid curve on Fig. 4). Also shown on the figure are the PEB values if all beacons were LOS (lower dotted line) and if the NLOS beacons were ignored (upper dashed line).

It can be seen that when β_m goes to 0, PEB converges to the PEB when all beacons are LOS, as expected since $\beta_m = 0$ corresponds to all beacons being LOS. On the other hand when β_m goes to infinity PEB converges to the upper line. This is also expected since the information from the NLOS beacons reduces as β_m grows larger: for $\beta_m \to +\infty$ their contribution is altogether ignored (as shown in Section IID). However it is interesting to note that the NLOS beacons can help significantly in reducing the PEB, especially when β_m is small (NLOS measurements have small biases) or when d is large (the standard deviation of the range measurements is large compared to the biases). Therefore the range information from NLOS beacons should not be dismissed, as it can greatly improve the localization accuracy. In particular, if there is an incentive in using as few beacons as possible to estimate the agent's position (e.g. minimization of the number of beacons deployed, energy conservation in communication, or computational complexity), these results can be used to decide which beacons to involve in the localization process.

B. Case Study 2: Mapping PEB Throughout an Area

For a practical system we may be interested in the quality of localization not just at one point, but over an area. Let us map the value of the PEB throughout a square area for 6 LOS beacons placed at the vertices of a polygon of radius $d = 10$ m (Fig. 5). This contour plot reveals that the center of the polygon is no longer the location with minimum PEB, contrary to the common conclusions in the literature based on a model where the range measurement variance does not depend on distance between agent and corresponding beacons [38]. In other words, when the beacons are so arranged, the agent should not expect to have optimal localization accuracy in the center of the polygon. The situation becomes all the more complicated when NLOS beacons are included.

Suppose that we desire the PEB to be below a certain threshold τ for all points in the area. If at some location we have PEB $> \tau$, then whatever position estimator is used, the localization accuracy will be above the required threshold (since the PEB is a lower bound on the estimator accuracy). In this case we say that the localization system is in outage at this location, and we define the outage probability for a given τ as

$$p_{\text{out}}(\tau) \triangleq \mathbb{P}\{\text{PEB} > \tau\}. \tag{48}$$

The outage probability tells us that as the agent moves through the area, with probability $p_{\text{out}}(\tau)$ the PEB will exceed the required threshold so that the localization accuracy will be unsatisfactory. If the threshold τ is chosen large enough, then the outage probability will approach 0, otherwise it will grow as more locations in the area will not meet the accuracy requirement. We illustrate this on Fig. 6 where we plot the relative frequency diagram of the PEB over a 20 m by 20 m area where 10 beacons are placed at the vertices of a polygon, with $\beta_m = 2$ m and $\rho = 0.3$. The area covered for PEB $> \tau$ represents the outage probability. Note that in most practical cases beacons will not

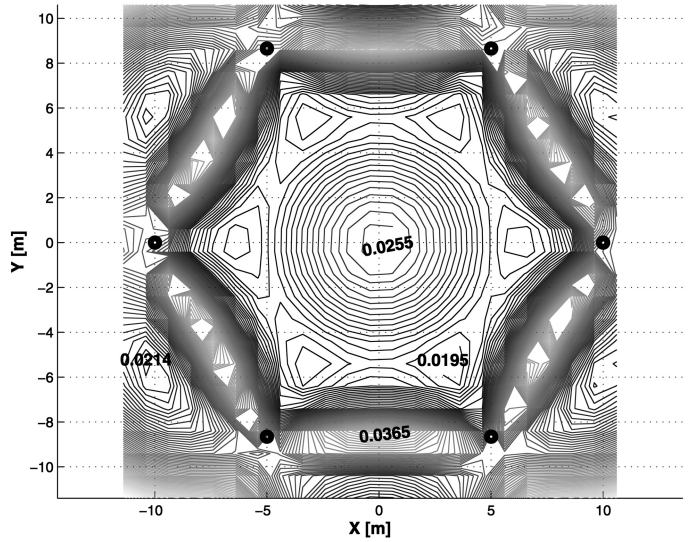

Fig. 5. Case 2: Contour map of PEB when 6 LOS beacons are placed at vertices of polygon with $d = 10$ m.

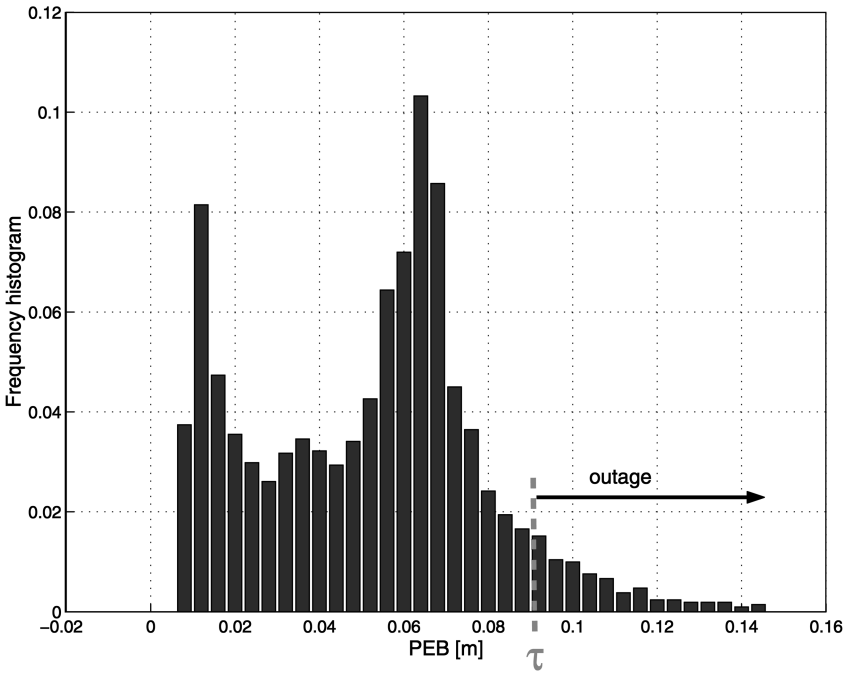

Fig. 6. Case 2: Frequency histogram of PEB over area for 10 beacons placed at vertices of polygon, where $\beta_m = 2$ m and $\rho = 0.3$. Area to right of τ represents outage probability.

remain LOS or NLOS for all possible target positions (exception made for particular cases). However, we assume here that this is the case in order to show the importance of the outage probability and the impact of NLOS beacons. Our approach remains valid in the more general case.

On Fig. 7 we plot the outage probability as a function of the threshold τ for $\rho = 0.3$ and different values of β_m. We also show $p_{out}(\tau)$ for the extreme cases when only the LOS beacons are taken into account ($\beta_m \to +\infty$, rightmost curve) or when all the beacons are LOS ($\beta_m = 0$, leftmost curve). The curves for positive values of β_m lie between these two. In addition, we can observe that for low τ the sensitivity of the outage probability to β_m becomes larger. If a certain accuracy threshold is desired, these curves can help determine whether more beacons should be deployed. In Table I we show the outage probability for different values of the threshold τ and β_m.

C. Case Study 3: Results with ϵ-Localization Accuracy Outage

In order to capture with a single number the quality of localization throughout the area, we define $\text{PEB}_{1-\epsilon}$, the ϵ-localization accuracy outage,

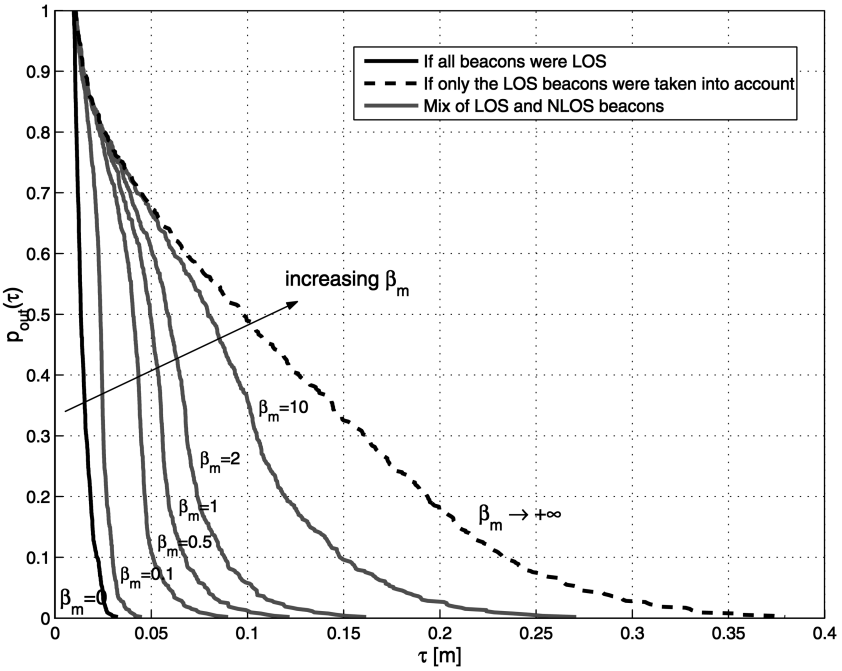

Fig. 7. Case 2: Outage probability over area of 10 beacons of Fig. 6 for $\beta_m = 0, 0.1, 0.5, 1, 2, 10$ m, and limit as $\beta_m \to +\infty$.

TABLE I
Outage Probability for Different Values of τ [m] and β_m [m]

	$\beta_m = 0.1$ m	$\beta_m = 1$ m	$\beta_m = 2$ m	$\beta_m \to +\infty$
$\tau = 0.05$ m	0.025	0.4	0.57	0.9
$\tau = 0.1$ m	$< 10^{-3}$	0.012	0.04	0.33
$\tau = 0.15$ m	$< 10^{-3}$	$< 10^{-3}$	$< 10^{-3}$	0.09

as the value of the threshold τ for which the outage probability is ϵ, that is

$$\epsilon = \mathbb{P}\{\text{PEB} > \text{PEB}_{1-\epsilon}\}. \tag{49}$$

In the remainder of this paper we consider $\epsilon = 0.1$, so that PEB_{90} gives a good indication of the performance we can expect 90% of the time as we move through the area. We plot PEB_{90} as a function of β_m for different values of ρ on Fig. 8, when 10 beacons are placed randomly in a 20 m by 20 m area. Since the beacons are placed randomly, results are averaged over 100 trials to form the curves of Fig. 8. It can be seen that the proportion of LOS and NLOS beacons has a significant impact on the PEB. If we have control over ρ, then we should try to increase it especially when β_m is large and the number of LOS is relatively small. In other words, increasing the proportion of LOS beacons in cluttered environments (if it is possible) will significantly improve the PEB throughout the area. This plot also tells us the performance loss if a beacon initially thought to be LOS turns out to be NLOS. For example notice the large increase in PEB between $\rho = 0.5$ and $\rho = 0.4$. This penalty grows for larger β_m and smaller ρ.

We now investigate the benefit of taking NLOS information into account, compared with the case where we neglect it. On Fig. 9 we plot the ratio between $\text{PEB}_{90}(+\infty)$ obtained by using only the LOS beacons and $\text{PEB}_{90}(\beta_m)$, obtained with both LOS and NLOS beacons. Large values of this ratio indicate that the use of NLOS beacons yields a large reduction in the PEB compared with using only the LOS ones. The results show that the information from NLOS beacons can lower the PEB by several factors. This is especially true when the number of LOS beacons is relatively small. Also, lower uncertainty in the bias provides larger improvements in the PEB, indicating that the information from NLOS beacons is more useful when β_m is small.

IV. CONCLUSION

We determined the PEB that describes the limit on the accuracy of localization using UWB beacons. We considered the dense cluttered environment in which range measurements can be positively biased, and where their variance depends on the distance between agent and corresponding beacons. The PEB derived is easy to compute and accounts for the geometric configuration of the system, the increase of measurement variance with distance, and the presence of positive biases with general statistical characterization.

We then investigated properties of this bound. We found that, contrary to results where the measurement variance is treated as constant [38], when the beacons are at the vertices of a regular polygon the minimum

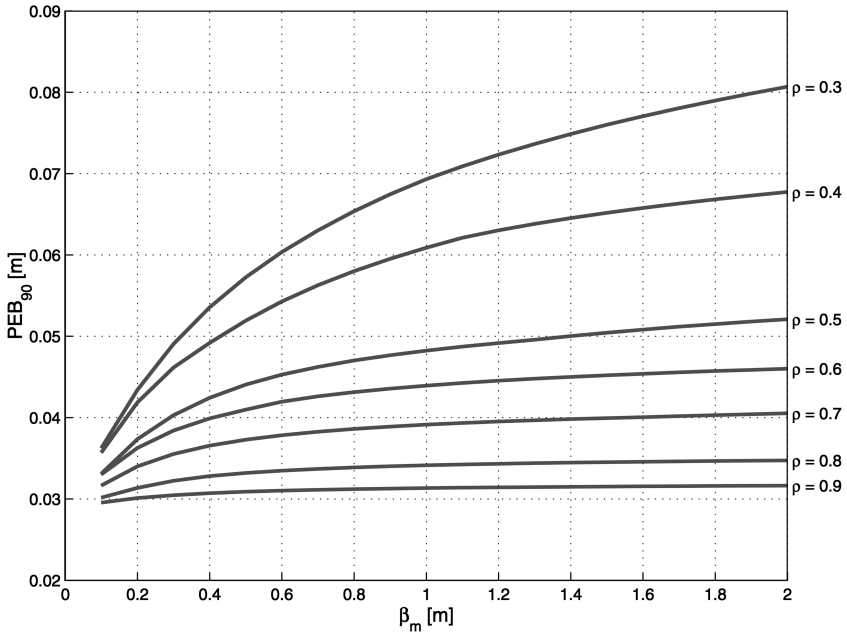

Fig. 8. Case 3: Average $\text{PEB}_{90}(\beta_{\text{m}})$ for 10 beacons randomly placed for different values of $\rho = n_{\text{LOS}}/n_{\text{B}}$.

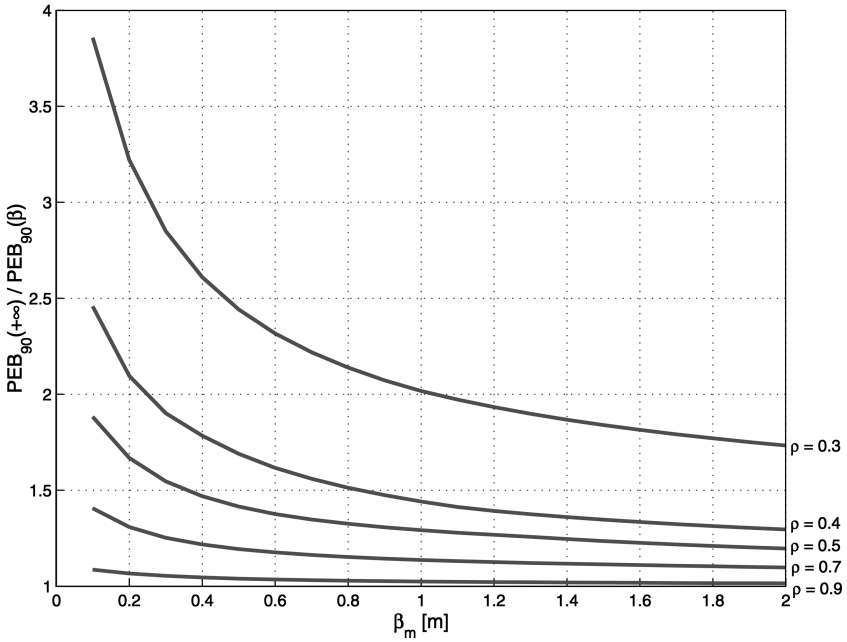

Fig. 9. Case 3: Average $\text{PEB}_{90}(+\infty)/\text{PEB}_{90}(\beta_{\text{m}})$. Large values indicate large reduction in PEB when NLOS beacons are taken into account.

value of the PEB is not found at the center. We also found that, in the case of a mix of LOS and NLOS beacons, the information from the NLOS beacons can be very valuable: taking the NLOS beacons into account often yields a significantly lower localization bound, especially in cluttered environments. We finally put forth the concept of localization accuracy outage, which can guide in making design decisions about the network such as the number and placement of the beacons, or whether to deploy additional beacons [32].

ACKNOWLEDGMENTS

The authors would like to thank H. Wymeersch, P. Pinto, and I. Keliher for their comments and careful reading of the manuscript. D. Dardari would also like to thank Prof. M. Chiani and O. Andrisano for their precious support.

APPENDIX

Referring to (16), let us examine the generic element in the sum of the upper left element of **J**. For

$i \neq j$ we have

$$\mathbb{E}_{\mathbf{r}}\left\{\frac{1}{f_i(r_i \mid \mathbf{p}_{\mathrm{A}})}\frac{1}{f_j(r_j \mid \mathbf{p}_{\mathrm{A}})}\frac{\partial f_i(r_i \mid \mathbf{p}_{\mathrm{A}})}{\partial x_{\mathrm{A}}}\frac{\partial f_j(r_j \mid \mathbf{p}_{\mathrm{A}})}{\partial x_{\mathrm{A}}}\right\}$$
$$= \mathbb{E}_{\mathbf{r}}\left\{\frac{1}{f_i(r_i \mid \mathbf{p}_{\mathrm{A}})}\frac{\partial f_i(r_i \mid \mathbf{p}_{\mathrm{A}})}{\partial x_{\mathrm{A}}}\right\} \cdot \mathbb{E}_{\mathbf{r}}\left\{\frac{1}{f_j(r_j \mid \mathbf{p}_{\mathrm{A}})}\frac{\partial f_j(r_j \mid \mathbf{p}_{\mathrm{A}})}{\partial x_{\mathrm{A}}}\right\} \quad (50)$$

since the measurements from beacons i and j are independent. We can write

$$\mathbb{E}_{\mathbf{r}}\left\{\frac{1}{f_i(r_i \mid \mathbf{p}_{\mathrm{A}})}\frac{\partial f_i(r_i \mid \mathbf{p}_{\mathrm{A}})}{\partial x_{\mathrm{A}}}\right\} = \int_{-\infty}^{+\infty}\frac{1}{f_i(r_i \mid \mathbf{p}_{\mathrm{A}})}\frac{\partial f_i(r_i \mid \mathbf{p}_{\mathrm{A}})}{\partial x_{\mathrm{A}}} f_i(r_i \mid \mathbf{p}_{\mathrm{A}})dr_i \quad (51)$$

$$= \int_{-\infty}^{+\infty}\frac{\partial f_i(r_i \mid \mathbf{p}_{\mathrm{A}})}{\partial x_{\mathrm{A}}}dr_i. \quad (52)$$

We know that $f_i(r_i \mid \mathbf{p}_{\mathrm{A}})$ is a continuous function of (r_i, x_{A}). It is also easy to show that its derivative $\partial f_i(r_i \mid \mathbf{p}_{\mathrm{A}})/\partial x_{\mathrm{A}}$ (see equation (18)) is also continuous, and that its absolute value is integrable in r_i for all x_{A}. We can therefore exchange the integral with the derivative so that

$$\int_{-\infty}^{+\infty}\frac{\partial f_i(r_i \mid \mathbf{p}_{\mathrm{A}})}{\partial x_{\mathrm{A}}}dr_i = \frac{\partial}{\partial x_{\mathrm{A}}}\int_{-\infty}^{+\infty} f_i(r_i \mid \mathbf{p}_{\mathrm{A}})dr_i = 0 \quad (53)$$

since $\int_{-\infty}^{+\infty} f_i(r_i \mid \mathbf{p}_{\mathrm{A}})dr_i = 1$. The same holds for the derivative with respect to y_{A}.

REFERENCES

[1] Spilker, J. J., Jr.
GPS signal structure and performance characteristics.
Journal of the Institute of Navigation, **25**, 2 (Summer 1978), 121–146.

[2] Low, Z. N., Cheong, J. H., Law, C. L., Ng, W. T., and Lee, Y. J.
Pulse detection algorithm for line-of-sight (LOS) UWB ranging applications.
IEEE Antennas and Wireless Propagation Letters, **4** (2005), 63–67.

[3] Falsi, C., Dardari, D., Mucchi, L., and Win, M. Z.
Time of arrival estimation for UWB localizers in realistic environments.
EURASIP Journal of Applied Signal Processing (special issue on Wireless Location Technologies and Applications), **2006** (2006).

[4] Dardari, D., Chong, C.-C., and Win, M. Z.
Analysis of threshold-based toa estimators in UWB channels.
In *Proceedings of the European Signal Processing Conference* (EUSIPCO 2006), Florence, Italy, Sept. 2006.

[5] Dardari, D., Chong, C.-C., and Win, M. Z.
Improved lower bounds on time-of-arrival estimation error in realistic UWB channels.
In *Proceedings of the IEEE International Conference on Ultra-Wideband* (ICUWB 2006), Waltham, MA, Sept. 2006.

[6] Gezici, S., Tian, Z., Giannakis, G., Kobayashi, H., Molisch, A., Poor, H., and Sahinoglu, Z.
Localization via ultra-wideband radios: A look at positioning aspects for future sensor networks.
IEEE Signal Processing Magazine, **22** (July 2005), 70–84.

[7] Lee, J.-Y., and Scholtz, R. A.
Ranging in a dense multipath environment using an UWB radio link.
IEEE Journal on Selected Areas of Communications, **20**, 9 (Dec. 2002), 1677–1683.

[8] Win, M. Z., and Scholtz, R. A.
On the robustness of ultra-wide bandwidth signals in dense multipath environments.
IEEE Communications Letters, **2**, 2 (Feb. 1998), 51–53.

[9] Win, M. Z., and Scholtz, R. A.
On the energy capture of ultra-wide bandwidth signals in dense multipath environments.
IEEE Communications Letters, **2**, 9 (Sept. 1998), 245–247.

[10] Cassioli, D., Win, M. Z., and Molisch, A. F.
The ultra-wide bandwidth indoor channel: From statistical model to simulations.
IEEE Journal on Selected Areas of Communication, **20**, 6 (Aug. 2002), 1247–1257.

[11] Win, M. Z., and Scholtz, R. A.
Characterization of ultra-wide bandwidth wireless indoor communications channel: A communication theoretic view.
IEEE Journal on Selected Areas of Communication, **20**, 9 (Dec. 2002), 1613–1627.

[12] Chong, C.-C., and Yong, S. K.
A generic statistical-based UWB channel model for high-rise apartments.
IEEE Transactions on Antennas Propagation, **53**, 8 (Aug. 2005), 2389–2399.

[13] Chong, C.-C., Kim, Y.-E., Yong, S. K., and Lee, S.-S.
Statistical characterization of the UWB propagation channel in indoor residential environment.
Wireless Communications and Mobile Computing, **5**, 5 (Aug. 2005), 503–512.

[14] Win, M. Z., and Scholtz, R. A.
Impulse radio: How it works.
IEEE Communications Letters, **2**, 2 (Feb. 1998), 36–38.

[15] Win, M. Z., and Scholtz, R. A.
Ultra-wide bandwidth time-hopping spread-spectrum impulse radio for wireless multiple-access communications.
IEEE Transactions on Communication, **48**, 4 (Apr. 2000), 679–691.

[16] Win, M. Z.
A unified spectral analysis of generalized time-hopping spread-spectrum signals in the presence of timing jitter.
IEEE Journal on Selected Areas of Communication, **20**, 9 (Dec. 2002), 1664–1676.

[17] Ridolfi, A., and Win, M. Z.
Ultrawide bandwidth signals as shot-noise: A unifying approach.
IEEE Journal on Selected Areas of Communication, (2006), to be published.

[18] Suwansantisuk, W., Win, M. Z., and Shepp, L. A.
On the performance of wide-bandwidth signal acquisition in dense multipath channels.
IEEE Transactions on Vehicle Technology, **54**, 5 (Sept. 2005).

[19] Zhang, Z., Law, C. L., and Guan, Y. L.
BA-POC-Based ranging method with multipath mitigation.
IEEE Antennas Wireless Propagation Letters, **4** (2005), 492–495.

[20] Zhang, Z., Law, C. L., and Guan, Y. L.
BA-POC-Based ranging method with multipath mitigation in the NLOS environment.
Microwave and Optical Technology Letters, **47**, 4 (Nov. 2005), 318–320.

[21] Yarlagadda, R., Ali, I., Al-Dhahir, N., and Hershey, J.
GPS GDOP metric.
IEE Proceedings—Radar, Sonar Navigation, **147**, 5 (May 2000), 259–264.

[22] Bickel, P. J., and Doksum, K.
Mathematical Statistics: Basic Ideas and Selected Topics (2nd ed.), vol. 1.
Upper Saddle River, NJ: Prentice-Hall, 2001.

[23] Chaffee, J., and Abel, J.
GDOP and the Cramer-Rao bound.
In *Proceedings of the Position, Location and Navigation Symposium* (PLANS), Las Vegas, NV, Apr. 1994, 663–668.

[24] Chang, C., and Sahai, A.
Estimation bounds for localization.
In *Proceedings of the IEEE Conference on Sensor and Ad Hoc Communications and Networks*, Santa Clara, CA, Oct. 2004, 415–424.

[25] Savvides, A., Garber, W., Adlakha, S., Moses, R., and Srivastava, M.
On the error characteristics of multihop node localization in ad-hoc sensor networks.
In *Proceedings of the Second International Workshop on Information Processing in Sensor Networks* (IPSN'03), Palo Alto, CA, Apr. 2003, 317–332.

[26] Larsson, E. G.
Cramér-Rao bound analysis of distributed positioning in sensor networks.
IEEE Signal Processing Letters, **11**, 3 (Mar. 2004), 334–337.

[27] Gavish, M., and Fogel, E.
Effect of bias on bearing-only target location.
IEEE Transactions on Aerospace and Electronic Systems, **26** (1990), 22–26.

[28] Qi, Y., and Kobayashi, H.
Cramér-Rao lower bound for geolocation in non-line-of-sight environment.
In *Proceedings of the International Conference on Acoustics, Speech, and Signal Processing*, Orlando, FL, May 2002, 2473–2476.

[29] Qi, Y., and Kobayashi, H.
On geolocation accuracy with prior information in non-line-of-sight environment.
In *Proceedings of the IEEE Vehicular Technology Conference* (VTC 2002), Vancouver, BC, Sept. 2002, 285–288.

[30] Qi, Y., Suda, H., and Kobayashi, H.
On time-of-arrival positioning in a multipath environment.
In *Proceedings of the 60th IEEE Vehicular Technology Conference* (VTC 2004-Fall), Los Angeles, CA, Sept. 26–29, 2004.

[31] Wang, H., Yip, L., Yao, K., and Estrin, D.
Lower bounds of localization uncertainty in sensor networks.
In *Proceedings of the International Conference on Acoustics, Speech, and Signal Processing*, Montreal, Canada, May 2004, 917–920.

[32] Jourdan, D. B., and Roy, N.
Optimal sensor placement for agent localization.
In *Proceedings of the IEEE/ION Conference on Position, Location, and Navigation* (PLANS), San Diego, CA, Apr. 2006.

[33] Jourdan, D. B., Deyst, J. J., Win, M. Z., and Roy, N.
Monte-Carlo localization in dense multipath environments using UWB ranging.
In *Proceedings of IEEE International Conference on Ultra-Wideband*, Zurich, Switzerland, Sept. 2005, 314–319.

[34] Tehoffo-Talom, F., Uguen, B., Plouhinec, E., and Chassay, G.
A site-specific tool for UWB channel modeling.
In *2004 International Workshop on Ultra Wideband Systems*, Kyoto, Japan, May 2004, 61–65.

[35] Borras, J., Hatrack, P., and Mandayam, N. B.
Decision theoritic framework for NLOS identification.
In *Proceedings of the IEEE Vehicular Technology Conference*, vol. 2, Ottawa, Canada, May 1998, 1583–1587.

[36] Venkatraman, S., and Caffery, J.
A statistical approach to non-line-of-sight BS identification.
In *Proceedings of the IEEE 5th International Symposium on Wireless Personal Multimedia Communications*, vol. 1, Honolulu, HI, Oct. 2002, 296–300.

[37] Gezici, S., Kobayashi, H., and Poor, H.
Non-parametric non-line-of-sight identification.
In *Proc. IEEE Vehicular Technology Conference*, vol. 4, Orlando, FL, Oct. 1998, 2544–2548.

[38] Levanon, N.
Lowest GDOP in 2-D scenarios.
IEE Proceedings—Radar, Sonar Navigation, **147**, 3 (Mar. 2000), 149–155.

Damien B. Jourdan (S'05—M'07) received an Engineering degree from the Ecole Centrale Paris in France, and went on to receive M.S. (2003) and Ph.D. (2006) degrees from the Massachusetts Institute of Technology in the Department of Aeronautics and Astronautics.

He is currently the senior research engineer at Athena Technologies, in Warrenton, VA. His interests lie in estimation, navigation, controls, and optimization.

Dr. Jourdan received the Best Student Paper award at the 2006 ION/IEEE Position, Location and Navigation Symposium (PLANS). He is a guest editor for the special issue of the *EURASIP Journal on Applied Signal Processing*, "*Cooperative Localization in Wireless Ad hoc and Sensor Networks*," to be published in 2008.

Davide Dardari received the Laurea degree in electronic engineering (summa cum laude) and the PhD degree in electronic engineering and computer science from the University of Bologna, Italy, in 1993 and 1998, respectively. In 1998, he joined the Dipartimento di Elettronica, Informatica e Sistemistica to develop his research activities in the area of digital communications.

Since 2005, he has been a Research Affiliate at Massachusetts Institute of Technology (MIT), Cambridge, USA. Now, he is an Associate Professor at the University of Bologna at Cesena, Italy, where he participates with WiLAB (Wireless Communications Laboratory). Recently, he has focused his activity on ultra-wide bandwidth (UWB) systems, ranging and localization techniques, as well as wireless sensor networks. He is Senior Member of the IEEE where he is the current secretary for the Radio Communications Committee of the IEEE Communication Society. He was co-chair of the Wireless Communications Symposium of the 2007 IEEE International Conference on Communications and of the 2006 IEEE International Conference on Ultra-Wideband.

Dr. Dardari currently serves as an Editor for *IEEE Transactions On Wireless Communications* and Lead Editor for the *EURASIP Journal on Advances in Signal Processing* (Special Issue on Cooperative Localization in Wireless Ad Hoc and Sensor Networks). He also serves as a reviewer for Transactions/Journals and Conferences, and as a TPC member for numerous international conferences.

Moe Z. Win (S'85—M'87—SM'97—F'04) received the B.S. degree (magna cum laude) from Texas A&M University, College Station, in 1987, and the M.S. degree from the University of Southern California (USC), Los Angeles, in 1989, both in Electrical Engineering. As a Presidential Fellow at USC, he received both an M.S. degree in Applied Mathematics and the Ph.D. degree in Electrical Engineering in 1998. Dr. Win is an Associate Professor at the Laboratory for Information & Decision Systems (LIDS), Massachusetts Institute of Technology (MIT). Prior to joining MIT, he spent five years at AT&T Research Laboratories and seven years at the Jet Propulsion Laboratory. His main research interests are the applications of mathematical and statistical theories to communication, detection, and estimation problems. Specific current research topics include location-aware networks, measurement and modeling of time-varying channels, design and analysis of multiple antenna systems, ultra-wide bandwidth (UWB) systems, optical transmission systems, and space communications systems.

Professor Win has been actively involved in organizing and chairing a number of international conferences. He served as the Technical Program Chair for the IEEE Conference on Ultra Wideband in 2006, the IEEE Communication Theory Symposia of ICC-2004 and Globecom-2000, and the IEEE Conference on Ultra Wideband Systems and Technologies in 2002; Technical Program Vice-Chair for the IEEE International Conference on Communications in 2002; and the Tutorial Chair for ICC-2009 and the IEEE Semiannual International Vehicular Technology Conference in Fall 2001. He served as the chair (2004-2006) and secretary (2002-2004) for the Radio Communications Committee of the IEEE Communications Society. Dr. Win is currently an Editor for *IEEE Transactions on Wireless Communications*. He served as Area Editor for *Modulation and Signal Design* (2003-2006), Editor for *Wideband Wireless and Diversity* (2003-2006), and Editor for *Equalization and Diversity* (1998-2003), all for the *IEEE Transactions on Communications*. He was Guest-Editor for the 2002 *IEEE Journal on Selected Areas in Communications* (Special Issue on Ultra-Wideband Radio in Multiaccess Wireless Communications).

Professor Win's recognitions include the Office of Naval Research Young Investigator Award (2003), the U.S. Presidential Early Career Award for Scientists and Engineers (2004), and the Laurea Honoris Causa from the University of Ferrara, Italy (2008). His papers have received numerous awards including the IEEE Antennas and Propagation Society's Sergei A. Schelkunoff Transactions Prize Paper Award (2003), the IEEE Wireless Communications and Networking Conference Best Paper Award (2007), the IEEE Vehicular Technology Conference Best Paper Award (2008), and the IEEE Communications Society's Guglielmo Marconi Best Paper Award (2008). In 2004, Professor Win was named Young Aerospace Engineer of the Year by the AIAA, and he received a Fulbright Foundation Senior Scholar Lecturing and Research Fellowship, and an Institute of Advanced Study Natural Sciences and Technology Fellowship. Of particular significance, he was honored with the IEEE Eric E. Sumner Award (2006), an IEEE Technical Field Award, for "pioneering contributions to ultra-wide band communications science and technology." Professor Win is an IEEE Distinguished Lecturer and an elected Fellow of the IEEE, cited for "contributions to wideband wireless transmission."